Journal of Thermal Analysis and Calorimetry (2020) 139:2913–2923
https://doi.org/10.1007/s10973-019-09198-1

Improving performance of AHU using exhaust air potential by applying exergy analysis

Rasool Kalbasi[1] · Farhad Izadi[1] · Pouyan Talebizadehsardari[2,3]

Received: 14 October 2019 / Accepted: 12 December 2019 / Published online: 20 January 2020

Abstract
In this study, the exergy analysis of an AHU equipped with a heat and exergy recovery unit was investigated. The equations obtained from energy and exergy balance were solved based on a program developed in engineering equation solver. Through the air-to-air heat exchanger, the energy is transferred from the fresh air to the exhaust one but the exergy is transferred from the exhaust air to the fresh one. Therefore, the cooling coil power consumption and irreversibility were reduced. The efficacy of installing an air-to-air heat exchanger is dependent on the temperature and relative humidity of the ambient. Based on the results, at the lowest ambient temperature and relative humidity, the power consumption is reduced by 10.8%, while in the highest ambient temperature and relative humidity, this figure was 33%. Under ambient conditions with low temperatures and high relative humidity, installation of heat recovery unit reduced the irreversibility by 5.18%, while in the highest temperature and lowest relative humidity this figure was 12.8%.

Keywords AHU · Irreversibility · Enthalpy air-to-air heat exchanger · Power consumption

List of symbols

C	Heat capacity (kJ kg^{-1} K^{-1})
Ex	Exergy (kJ kg^{-1})
h	Enthalpy (kJ kg^{-1})
Q_s	Sensible heat exchange (kW)
Q_l	Latent heat exchange (kW)
R_a	Air constant (kJ kg^{-1} K^{-1})
R_v	Vapor constant (kJ kg^{-1} K^{-1})
s	Entropy (kJ kg^{-1} K^{-1})
T	Temperature (K)

Superscripts

Air-to-air	Heat recovery unit
cc	Cooling coil
hc	Heating coil
mixing	Mixing box
room	Conditioned space

Greek letters

φ	Relative humidity
ω	Humidity ratio $\left(\frac{kg_v}{kg_a}\right)$
ε	Effectiveness

Subscripts

a	Point a (outlet of air-to-air heat exchanger)/air
c	Point c (outlet of cooling coil)
Co	Water outlet from cooling coil
Ci	Cooling coil inlet water
cond	Condensation
des	Destroyed
e	Point e (exhaust air)
hi	Heating coil inlet water
ho	Heating coil outlet water
f	Point f (fresh air)
m	Point m (mixing)
r	Point r (return air)
s	Point s (supply air)
0	Reference condition

✉ Pouyan Talebizadehsardari
ptsardari@tdtu.edu.vn

[1] Department of Mechanical Engineering, Najafabad Branch, Islamic Azad University, Najafabad, Iran

[2] Department for Management of Science and Technology Development, Ton Duc Thang University, Ho Chi Minh City, Vietnam

[3] Faculty of Applied Sciences, Ton Duc Thang University, Ho Chi Minh City, Vietnam

Introduction

Almost half of the building energy demand is consumed by the HVAC system to maintain the ventilation requirements [1–4]. To date, many efforts have been made to reduce energy consumption in the HVAC system [5, 6]. One of the ways to reduce energy consumption is to use energy recovery techniques [7]. Air-to-air heat recovery is a device that can be used to recover energy [8]. In the enthalpy air-to-air heat exchanger, sensible energy (heat) and latent energy (vapor) are transmitted, while in the sensible air-to-air heat exchanger sensible heat is transferred from the hot stream to the cold stream [8]. More detail about the air-to-air heat exchanger is reported in Ref. [9].

Exergy analysis is a brilliant technique that accentuates the inefficiencies through the process [10–12]. The exergy analysis tells designers how far the system is away from its ideal state. If the exergy loss or irreversibility is zero, the process or cycle is ideal. The greater the irreversibility, the greater the deviation than the ideal state [13]. For comprehensive detail of exergy analysis utilization in the building, readers are referred to [14–17]. The first law of thermodynamics deals with the quantity of energy exchanged at the boundary, while the second law refers to the energy quality. The second law is concerned with the degradation of the work potential of the energy and can help designer to analyze and optimize the HVAC process. Various numerical approaches are applied by researchers to model various scientific processes [18–41]. Many exergy studies for example heat pumps [42–44], boilers [45], energy storage systems [46–48], HVAC [49–51], cooling system [52–68] and building envelope [69–71] have been conducted on building to decrease the building energy consumption.

In [44], the authors studied the heat pump (a ground source type) to utilize it in the building. They presented five control strategies to ameliorate the unit performance. Results revealed that the best strategies can decrease energy consumption and irreversibility which in turn increase the exergy efficiency and COP, respectively. The exergy analysis based on the connective thinking approach has been studied by Dovjak et al. [69]. Results indicated that the exergy consumption through the building envelope decreases due to the increase in thermal insulation resistance. Razmara et al. [72] performed the exergy analysis on building HVAC. They used the model predictive control (MPC) technique instead of traditional on–off controller. The results inferred that the MPC technique reduced the exergy destruction and energy consumption of the building HVAC up to 22% and 356%, respectively. Khalid et al. [73] performed the exergy analysis on three developed heating and cooling system in the residential building. The results showed that system operated by natural gas and vapor absorption chiller had priority over the other proposed systems. The first efficiency of the best system was 27.5%. The photovoltaic (PV) and solar thermal operated with vapor-compression chiller had the lowest first efficiency (19.9%) and highest second efficiency (3.9%). Sayadi et al. [74] applied the exergy analysis on the large complex building and affirmed that the efficiency of the second law is very low (approximately 4%). Based on the exergy analysis, energy conversion systems account for the largest share (54%) in exergy losses. Caliskan et al. [75] proposed a novel desiccant air cooling. It consists of subsections such as a desiccant wheel, evaporative type of cooler and finally sensible wheel. They showed that the desiccant wheel has the highest share of exergy destruction (42.78%).

In this study, the effects of using enthalpy air-to-air heat exchanger on the second law were investigated. In the enthalpy, air-to-air heat recovery unit was installed at the AHU inlet and fresh air is pre-cooled through transferring sensible and latent heat to the exhaust air. Through the air-to-air heat exchanger, energy is transferred from the fresh air to the exhaust one but the exergy is transferred from the exhaust air to the fresh one. To evaluate the usefulness of heat exchanger installation, the exergy balance equations are developed. Irreversibility through the various components has been measured by solving the exergy balance equations based on a program developed in EES. The exergy balance results demonstrate the change made in the deviation of the system from its ideal state by adding the heat exchanger.

Description of the system

The AHU that has shown in Fig. 1 is utilized to satisfy the conditioned space ventilation requirements. In summer, the air temperature of the exterior (point f) is higher than the air temperature of the interior (point r); hence, cooling coil is required to reduce the air temperature of the exterior. But the presence of a cooling coil causes many changes in the relative humidity of the air. The heating coil is used to reduce relative humidity changes.

In other words, the heating coil is used to provide adequate humidity content in the conditioned space. As seen, a portion of the return air is recirculated and the rest is exhausted. In other words, energy and exergy are transferred from the AHU to the ambient. Exhaust air energy and exergy can be utilized in the heat recovery unit installed at the AHU entrance.

Exergy analysis

In this study, the studied AHU is of constant air volume (CAV) type. In this type of AHU, the required mass flow rates of fresh air and supply air should be determined through the following equations:

$$\dot{m}_{\mathrm{s}}^{\mathrm{air}} = \frac{\text{air changes per hour} \times \text{space volume}}{3600 \times \text{specific volume}} \tag{1}$$

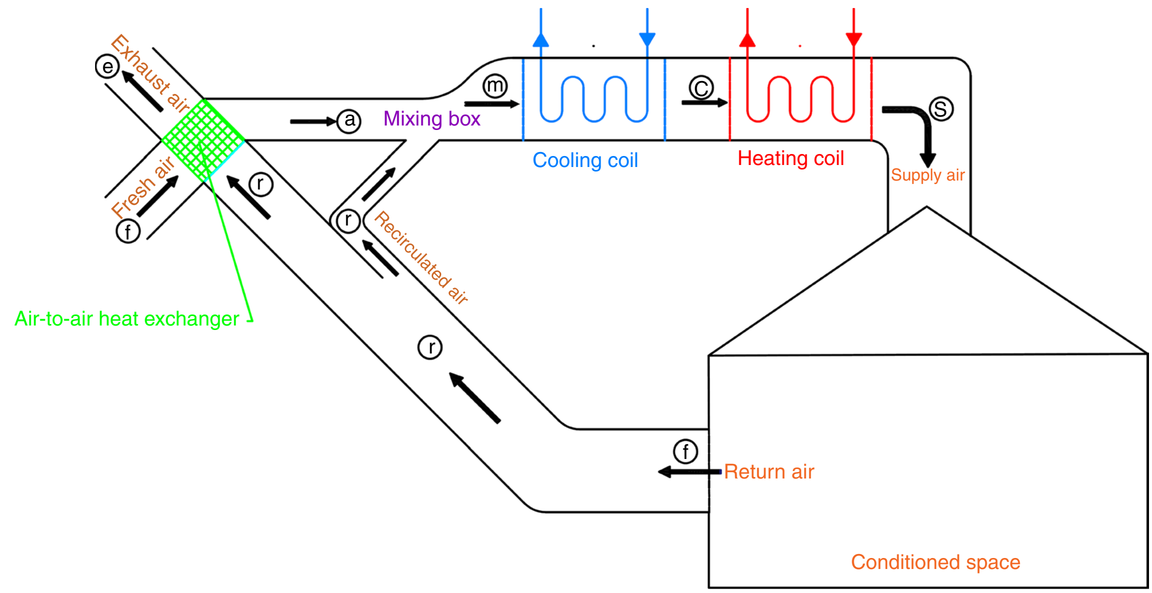

Fig. 1 Modified AHU

$$\dot{m}_{\mathrm{f}}^{\mathrm{air}}=\frac{\text{people number}\times\text{required fresh air per person}}{1000\times\text{specific volume}}\tag{2}$$

The exergy destruction through the heat recovery unit is obtained using exergy balance. Applying the exergy balance method, heat recovery unit exergy destruction is written as follow:

$$\dot{m}_{\mathrm{f}}^{\mathrm{air}}\,\mathrm{Ex}_{\mathrm{f}}+\left(\dot{m}_{\mathrm{r}}^{\mathrm{air}}-\dot{m}_{\mathrm{re}}^{\mathrm{air}}\right)\mathrm{Ex}_{\mathrm{r}}-\dot{m}_{\mathrm{a}}^{\mathrm{air}}\,\mathrm{Ex}_{\mathrm{a}}-\dot{m}_{\mathrm{e}}^{\mathrm{air}}\,\mathrm{Ex}_{\mathrm{e}}-\mathrm{Ex}_{\mathrm{des}}^{\mathrm{air\,to\,air}}=0\tag{3}$$

The mixing box exergy destruction is obtained by performing exergy balance:

$$\dot{m}_{\mathrm{a}}^{\mathrm{air}}\,\mathrm{Ex}_{\mathrm{a}}+\dot{m}_{\mathrm{re}}^{\mathrm{air}}\,\mathrm{Ex}_{\mathrm{r}}-\dot{m}_{\mathrm{m}}^{\mathrm{air}}\,\mathrm{Ex}_{\mathrm{m}}-\mathrm{Ex}_{\mathrm{des}}^{\mathrm{mixing}}=0\tag{4}$$

The cooling coil exergy destruction is obtained using the following equation:

$$\begin{aligned}&\dot{m}_{\mathrm{m}}^{\mathrm{air}}\,\mathrm{Ex}_{\mathrm{m}}+\dot{m}_{\mathrm{ci}}^{\mathrm{water}}\,\mathrm{Ex}_{\mathrm{ci}}-\dot{m}_{\mathrm{c}}^{\mathrm{air}}\,\mathrm{Ex}_{\mathrm{c}}-\dot{m}_{\mathrm{co}}^{\mathrm{water}}\,\mathrm{Ex}_{\mathrm{co}}\\&\quad-\dot{m}_{\mathrm{cond}}\,\mathrm{Ex}_{\mathrm{cond}}-\mathrm{Ex}_{\mathrm{des}}^{\mathrm{cc}}=0\end{aligned}\tag{5}$$

where $\mathrm{Ex}_{\mathrm{cond}}$ denotes exergy of condensation vapor and $\dot{m}_{\mathrm{cond}}$ is the vapor condensation mass flow rate.

Applying the exergy balance on the heating coil yields:

$$\dot{m}_{\mathrm{c}}^{\mathrm{air}}\,\mathrm{Ex}_{\mathrm{c}}+\dot{m}_{\mathrm{hi}}^{\mathrm{water}}\,\mathrm{Ex}_{\mathrm{hi}}-\dot{m}_{\mathrm{s}}^{\mathrm{air}}\,\mathrm{Ex}_{\mathrm{s}}-\dot{m}_{\mathrm{ho}}^{\mathrm{water}}\,\mathrm{Ex}_{\mathrm{ho}}-\mathrm{Ex}_{\mathrm{des}}^{\mathrm{hc}}=0\tag{6}$$

where $\dot{m}_{\mathrm{hw}}$ denotes the mass flow rate of the hot water. Moreover, the exergy loss in the conditioned space is obtained as follows:

$$\dot{m}_{\mathrm{s}}^{\mathrm{air}}\,\mathrm{Ex}_{\mathrm{s}}-\dot{m}_{\mathrm{r}}^{\mathrm{air}}\,\mathrm{Ex}_{\mathrm{r}}-\mathrm{Ex}_{\mathrm{des}}^{\mathrm{room}}=0\tag{7}$$

The exergy of moist air (Eq. 8), distilled water (Eq. 9) and hot and cold water (Eq. 10) is required to perform an exergy analysis. These parameters are as follows [76]:

$$\begin{aligned}\mathrm{Ex}_{\mathrm{humid\ air}}=&\left(c_{\mathrm{p,a}}+\omega c_{\mathrm{p,v}}\right)\left(T-T_0-T_{\mathrm{o}}\ln\left[\frac{T}{T_{\mathrm{o}}}\right]\right)\\&+(1+1.608\omega)R_{\mathrm{a}}T_{\mathrm{o}}\ln\frac{P}{P_{\mathrm{o}}}+R_{\mathrm{a}}T_{\mathrm{o}}\\&\left[(1+1.608\omega)\ln\frac{1+1.608\omega}{1+1.608\omega_{\mathrm{o}}}+1.608\omega\ln\frac{\omega}{\omega_{\mathrm{o}}}\right]\end{aligned}\tag{8}$$

$$\mathrm{Ex}_{\mathrm{cond}}=h_{\mathrm{f}}-h_{\mathrm{f0}}-T_0(s_{\mathrm{f}}-s_{\mathrm{f0}})-R_{\mathrm{v}}T_0\ln(\varphi_0)+v_{\mathrm{f}}(P-P_{\mathrm{sat}})\tag{9}$$

$$\mathrm{Ex}_{\mathrm{hot\ and\ cold\ water}}=h_{\mathrm{f}}-h_{\mathrm{f0}}-T_0(s_{\mathrm{f}}-s_{\mathrm{f0}})\tag{10}$$

where s_{f0} and h_{f0} denote the water entropy and enthalpy at ambient temperature, φ_0 and ω_0 are the ambient relative humidity and humidity ratio.

The first and second laws of thermodynamic efficiencies are calculated from Eqs. (11) and (12), respectively.

$$\eta_{\mathrm{I}}=\frac{Q_{\mathrm{s}}+Q_{\mathrm{l}}}{\underbrace{Q^{\mathrm{cc}}}_{\text{cooling coil power}}+\underbrace{Q^{\mathrm{hc}}}_{\text{heating coil power}}}\tag{11}$$

$$\eta_{\mathrm{II}}=1-\frac{\text{total destroyed exergy}}{\text{input exergy}}\tag{12}$$

In Eq. (12), the total destroyed exergy is equal to the sum of irreversibility in each control volume:

Total destroyed exergy

$$= \mathrm{Ex}_{\mathrm{des}}^{\mathrm{air\,to\,air}} + \mathrm{Ex}_{\mathrm{des}}^{\mathrm{mixing}} + \mathrm{Ex}_{\mathrm{des}}^{\mathrm{cc}} + \mathrm{Ex}_{\mathrm{des}}^{\mathrm{hc}} + \mathrm{Ex}_{\mathrm{des}}^{\mathrm{room}}. \tag{13}$$

Results

As mentioned, AHU is used to satisfy the comfort requirements. Consider a conference hall with a volume of $40 \times 20 \times 8\ \mathrm{m}^3$ and the capacity of 800 people under the ambient thermodynamic properties of 22 °C and 40%. The conditioned space is under outdoor conditions with a temperature of 35 °C and a relative humidity of 50%. To meet comfort conditions, number of air changes per hour is 6 and required fresh air per person is selected 8 L s^{-1} [77]. For each person, the latent heat gain of 40 W and sensible heat gain of 100 W are considered. Due to the difference of thermodynamic properties between the inside (conditioned space) and outside (ambient), sensible heat gain of 120 kW and latent heat gain of 32 kW are transferred from the outside into the inside.

The heating process is accomplished using a heating coil equipped with hot water at the flow rate of 1.63 kg s^{-1} and temperature of 60 °C. The cooling process is performed by a cooling coil equipped with chilled water at temperature and mass flow rate of 6 °C and 15 kg s^{-1}.

According to the ventilation requirements, the fresh air mass flow rate should be 7 kg s^{-1}. Depending on the number of air changes per hour, the mass flow rate of supply air is calculated to be 12.46 kg s^{-1}; hence, the recirculated air mass flow rate is 5.46 kg s^{-1}. In other words, about 43% of the returning air is recirculated to AHU and 57% is exhausted. To meet the comfort requirements, supply air at temperature of 285.1 K and humidity ratio of 66.8% must be supplied. To change the ambient air thermodynamic properties (35 °C, 50%) to the supply thermodynamic properties of 285.1 K and 66.8%, the power consumption of the cooling and heating coils is 524 and 75.34 kW, respectively. According to Eq. (11), the first law efficiency is 25.36%. From the viewpoint of the second law, the exergy losses in mixing box, cooling coil, heating coil and ventilation space are 3.176, 10.28, 11.45 and 9.38 kW, respectively. Therefore, the total loss is 34.29 kW. The highest exergy losses are related to the heating coil and cooling with the respective losses of 33.33% and 29.97%. Finally, applying Eq. (12), the efficiency of the second law is 65%.

Now, the heat recovery unit is added to the base AHU and energy and exergy analysis is applied on the various parts. The sensible effectiveness of 0.7 and latent effectiveness of 0.5 for the enthalpy air-to-air heat exchangers are selected [78]. Performing energy calculations on the modified AHU, the power consumption of the heating and cooling coils will be 75.5 and 375.76 kW, respectively. Therefore, the total power consumption of the modified AHU is approximately 451.26 kW. A comparison of total power consumption between the modified AHU (451.26 kW) and the base AHU (599.34 kW) affirms that the total power consumption is reduced by 24.7%. Finally, owing to the reduction in power consumption, the first efficiency is enhanced by 32.8%.

The modified AHU exergy analysis is shown in Fig. 2. As shown in Fig. 2, the exergy losses in the air-to-air heat exchanger, mixing box, cooling coil, heating coil and ventilation space are 3.422, 1.067, 6.078, 11.47 and 9.38 kW, respectively. Therefore, the total loss is 31.418 kW. The highest exergy losses are related to the heating coil and ventilation space with the respective losses of 36.5% and 29.9%. The heat transfer process at the high-temperature difference between the input air and the water inside the heat exchanger tubes causes a considerable amount of exergy loss.

Installation of the enthalpy air-to-air heat exchanger also affects the second law analysis. Based on the results, the exergy losses of the system change from 34.38 to 31.418 kW (8.6% reduction) due to the installation of the heat exchanger. Therefore, the second law efficiency increases from 65 to 68%. The reduction in exergy losses

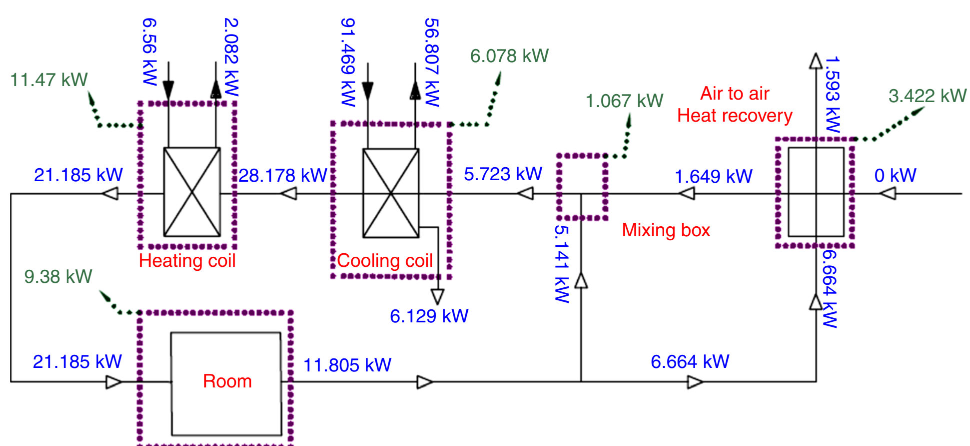

Fig. 2 Exergy balance for AHU with heat recovery

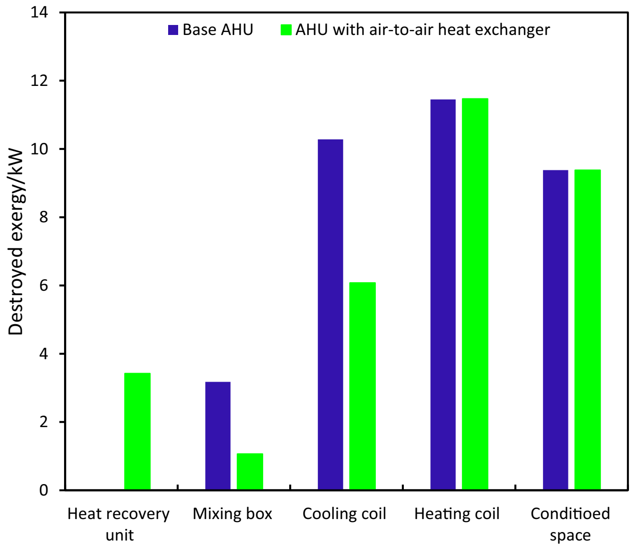

Fig. 3 Irreversibility through each component

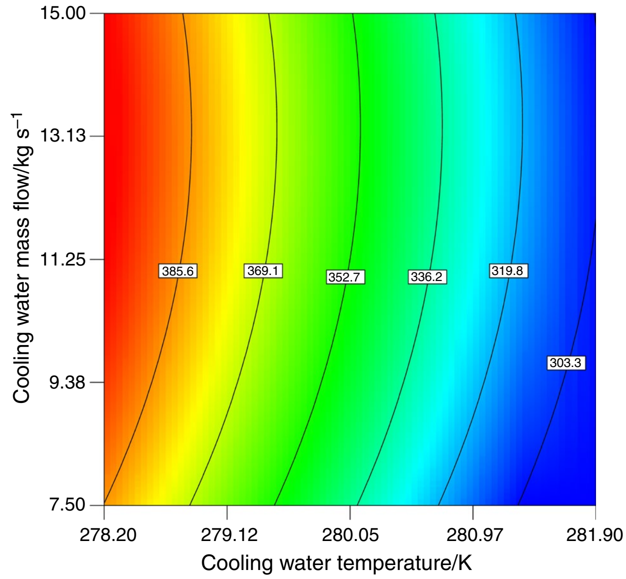

Fig. 4 Variations of cooling coil power with respect to the temperature and chilled water flow rate

can be due to the reduction in cooling coil power. Installing the enthalpy air-to-air heat exchanger reduced the power of the cooling coil, which in turn decreases the exergy losses. In general, after installing an air-to-air heat exchanger, the required cooling coil power and exergy losses are decreased by 148.2 kW and 2.88 kW, respectively.

Figure 3 compares the irreversibility of the base AHU and the modified one. Since the energy recovery unit is installed before the cooling coil, it affects the mixing box and the cooling coil. Installing heat recovery unit causes the inlet air to cool down, thus reducing the inlet air temperature at point a (Fig. 1). Hence, the temperature at points (a) and (r) (Fig. 1) gets closer and somehow the temperature difference decreases. The lower the temperature difference, the lower the irreversibility. Therefore, the irreversibility through the mixing box reduces. It was mentioned that using heat recovery unit reduces the power consumption of the cooling coil. Reducing the power of the cold coil will decrease the irreversibility as shown in Fig. 3.

The thermodynamic conditions of the cooling coil outlet and (point c) the supply air (point r in Fig. 1) are determined by equations that do not relate to temperature of point (a) (Fig. 1); hence, using of heat recovery unit does not affect the irreversibility through the heating coil and conditioned space.

In the following, the effect of various parameters on the usefulness of the adding heat recovery unit is examined.

Effects of chilled water temperature and mass flow rate

The required power of the cooling coil is a function of the chilled water temperature and mass flow rate. The variations of the cooling coil power consumption are shown in Fig. 4. As the cold water temperature decreases, the cooling coil load increases. Because as the cold water temperature decreases, the temperature difference between the air passing through the coil and the water inside the cooling coil increases; hence, the cooling coil load rises.

On the other hand, the higher the temperature difference, the greater the irreversibility. Therefore, as the cold water temperature decreases, the cooling coil irreversibility is also expected to increase (Fig. 5).

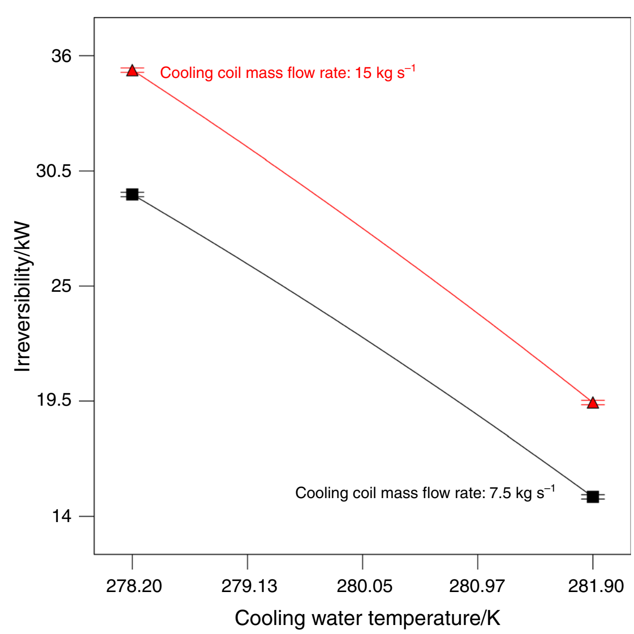

Fig. 5 Variations of irreversibility through the cooling coil

The chilled water outlet temperature is always warmer than the chilled water inlet temperature. In other words, there is a temperature difference between inlet and outlet cold water. As the chilled water mass flow rate increases, the temperature difference decreases. Clearly, the surface temperature of the cooling coil is colder, and therefore more vapor will be condensed. Hence, the cooling coil load increase as the chilled mass flow rate rises. This trend is shown in Fig. 4. As the power of the cooling coil increases, the irreversibility also rises. As shown in Fig. 5, with increasing chilled water mass flow rate, the irreversibility increases. As mentioned earlier, the cooling coil power increase as the chilled water flow rate increases. For this reason, the irreversibility in cooling coil and consequently the total irreversibility increase. On the other hand, inlet exergy to the system increases with the chilled water flow rate increase. However, the ratio of the input exergy increase is larger than the loss exergy increase; therefore, the $\frac{\text{total exergy loss}}{\text{input exergy}}$ fraction will reduce. Consequently, according to Eq. (12), the second law efficiency increases as shown in Fig. 6. It is necessary to mention that the increase in irreversibility affirms that the behavior of the system from the viewpoint of the second law deviates from its ideal state as the chilled water flow rate increases.

Effects of chilled water temperature and mass flow rate

As can be seen in Fig. 1, the power of the heating coil depends on the difference between the enthalpy of the cooling coil outlet air (h_c) and the enthalpy of the supply air (h_s). Parameter (h_s) is obtained from the thermodynamic analysis of the conditioned space. In other words, the power of the heating coil does not affect it. Parameter (h_c) is also obtained using the ε - NTU technique. In other words, the power of the heating coil depends only on the values of (h_c) and (h_s) and remains constant. Therefore, mass flow and temperature of the hot water have no impact on the first law efficiency. Exergy losses increase slightly in the heating coil in accordance with Eq. (6) as the hot water flow rate increases. As a result, the total exergy loss increases and the second law efficiency reduces slightly.

Effects of ambient conditions

Ambient conditions (temperature and relative humidity) affect the cooling and heating loads which in turn affect the irreversibility through them. In Fig. 7, the ambient conditions efficacy on the power consumption and the first efficiency are shown.

The inlet air enthalpy is dependent on relative humidity and temperature. The increase in temperature or relative humidity leads to an increase in enthalpy content. The more the enthalpy content, the higher the difference in energy content between the exterior and interior which in turn increases the power consumption and decreases the first law efficiency. This trend is shown in Fig. 7.

Note that the more the power consumption, the more irreversibility. Another reason for the increase in exergy losses is the increase in the exergy losses in the heat recovery unit. Exergy losses in the heat recovery unit are due to the temperature and humidity differences between return and fresh air streams. The more difference, the higher the exergy loss. The humidity difference between the fresh and return air increases

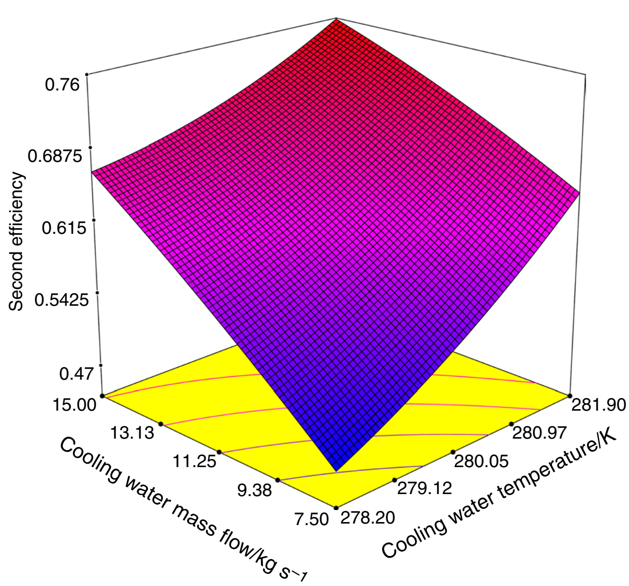

Fig. 6 Variations of the second law efficiency

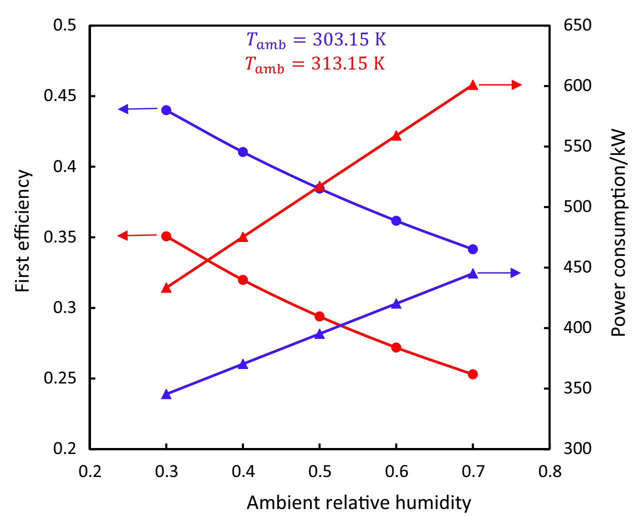

Fig. 7 Ambient conditions efficacy on the first efficiency and power consumption

as the relative humidity of the ambient increases. Therefore, the exergy loss of the heat recovery unit increases.

In Fig. 8, it is found that at the lowest ambient temperature power consumption and irreversibility have the lowest values. The same is correct for the relative humidity of the exterior, and at the lowest relative humidity, irreversibility and power consumption have the lowest values. Therefore, at the lowest exterior relative humidity and temperature, the modified AHU has the lowest power consumption and is closer to its ideal behavior.

Recovered power is a function of ambient conditions. Through the enthalpy units, the latent energy, as well as the sensible energy, is transferred from the fresh air (with the ambient thermodynamic properties) to the exhaust air (with the conditioned thermodynamic properties). Given that indoor (conditioned space) conditions are constant, any changes in ambient conditions can affect recovered power. As shown in Fig. 9, with the increase in ambient temperature and relative humidity, the recovered power increases. In other words, in hot and humid regions, the efficacy of

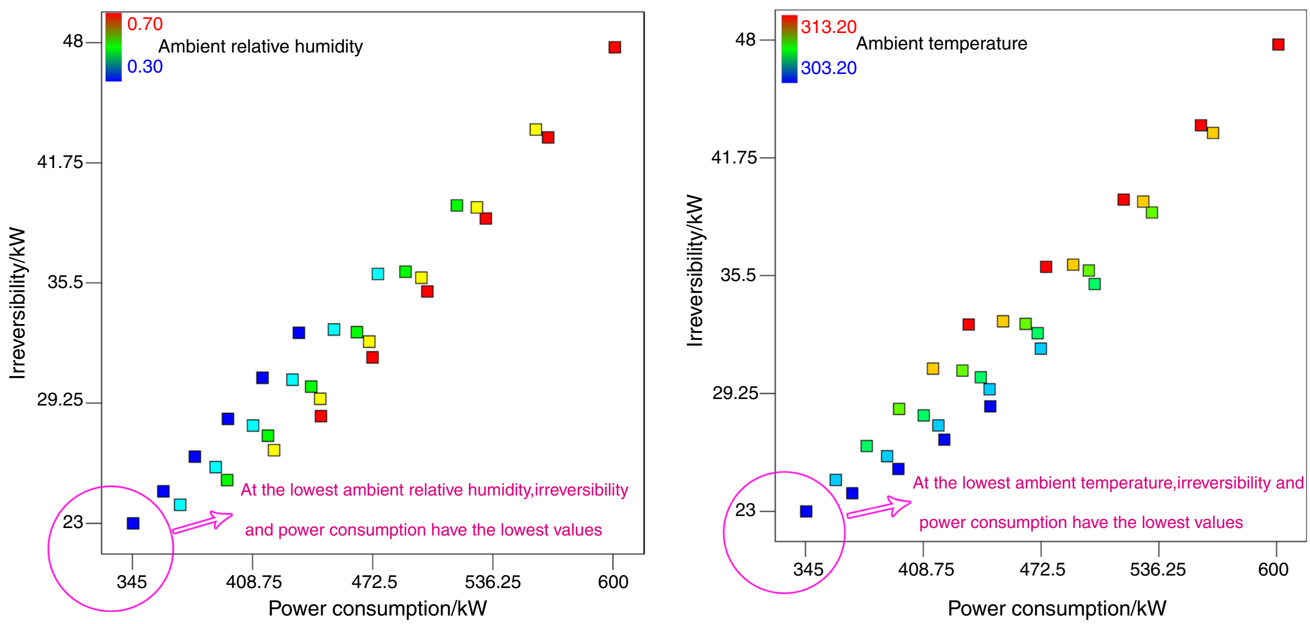

Fig. 8 Efficacy of exterior temperature and relative humidity on the exergy losses

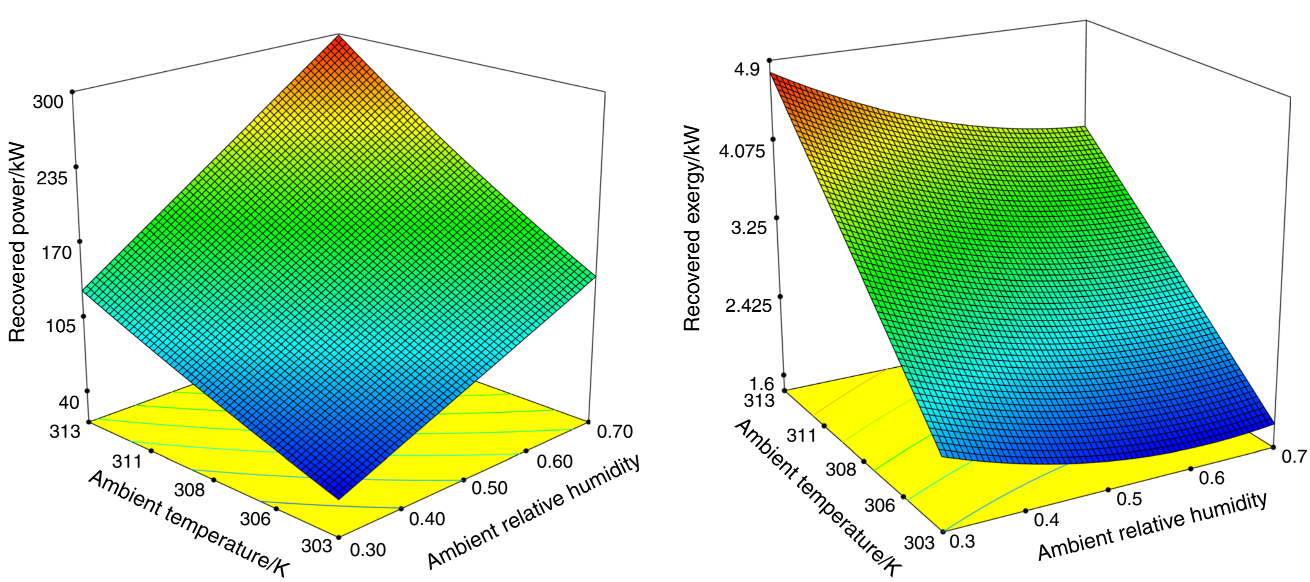

Fig. 9 Variations of recovered power and recovered exergy in the enthalpy air-to-air heat exchanger in terms of ambient conditions

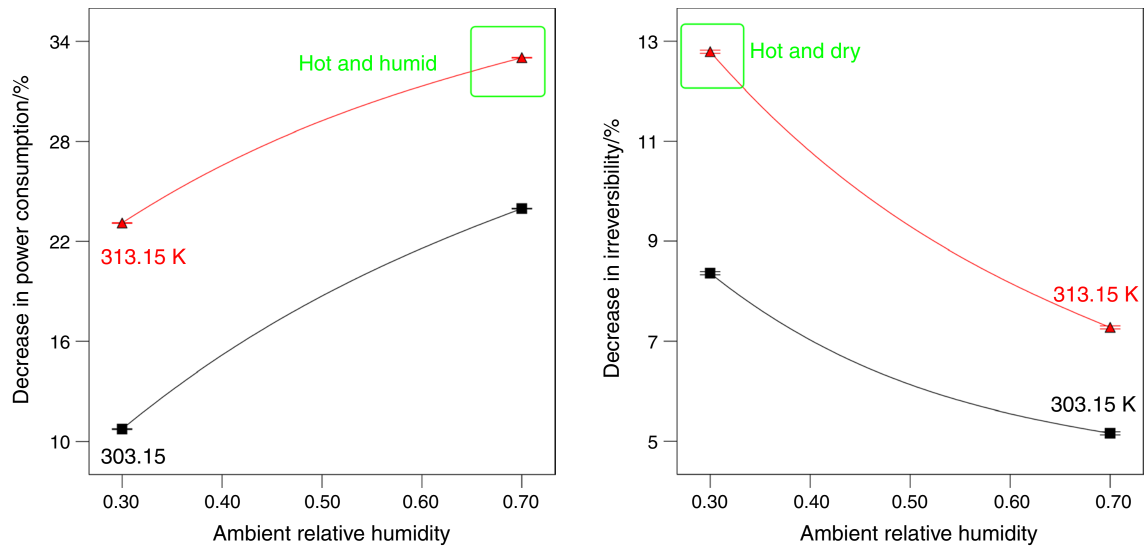

Fig. 10 Decrease in power consumption and irreversibility at various ambient conditions

installing the heat recovery unit on the recovered power appears to be greater.

Figure 9 shows the recovered exergy in terms of ambient conditions. It demonstrates that the using of enthalpy air-to-air heat exchanger on exergy recovery has the greatest effect at ambient with low relative humidity and high. Also, it has the least effect at a low temperature and high relative humidity.

Now the question is whether installing a heat recovery unit in hot and humid is preferable or in hot and dry one?

In Fig. 10, the effects of adding hear recovery unit on the irreversibility reduction and power consumption reduction are shown.

As shown in Fig. 10, installing a heat recovery unit, the energy consumption is reduced by at least 10.8% (in ambient with hot and dry climate) and maximum by 33% (hot and humid one). Moreover, incorporating heat recovery unit decreases the irreversibility at least 5.18% (in ambient with hot and dry climate) and maximum up to 12.8% (hot and humid one).

Conclusions

In this study, the effects of using the enthalpy heat recovery unit on the second law were investigated. In the enthalpy, the unit was installed at the AHU inlet and fresh air is pre-cooled through transferring sensible and latent heat to the exhaust air. Through the enthalpy unit, the energy is transferred from the fresh air to the exhaust one but the exergy is transferred from the exhaust air to the fresh one. Therefore, the power consumption of the cooling coil was reduced (owing to the pre-cooling). In addition, due to exergy recovery in the air-to-air heat exchanger, the total irreversibility is decreased. It was found that the exergy losses were 34.288 kW, which is 8.7% lower than the base AHU irreversibility (31.417 kW). Owing to the less total exergy losses, the efficiency of the second law enhanced from 0.65 to 0.68 (4.6% improvement).

The ambient conditions have an impact on the recovered exergy. At the ambient temperature of 303.2 K, as the ambient relative humidity changes from 0.3 to 0.7, using enthalpy air-to-air heat exchanger changes the recovered exergy from 2.157 to 1.645 kW. When relative humidity is 0.5, it is found that with the increase in temperature from 303.2 to 313.2 K (10 K increase), the recovered exergy increases from 1.721 to 4.058 kW. In other words, the amount of recovered exergy is increased by a decrease in ambient relative humidity or an increase in ambient temperature.

References

1. Afrand M, Shahsavar M, Talebizadeh Sardari P, Sopian K, Salehipour H. Energy and exergy analysis of two novel hybrid solar photovoltaic geothermal energy systems incorporating a building integrated photovoltaic thermal system and an earth air heat exchanger system. Solar Energy 2019;188:83–95.
2. Li ZX, Shahsavar A, Al-Rashed AAAA, Kalbasi R, Afrand M, Talebizadehsardari P. Multi-objective energy and exergy optimization of different configurations of hybrid earth-air heat exchanger and building integrated photovoltaic/thermal system. Energy Convers Manag 2019;195:1098–110.
3. Gao W, Moayedi H, Shahsavar A. The feasibility of genetic programming and ANFIS in prediction energetic performance of a building integrated photovoltaic thermal (BIPVT) system. Solar Energy 2019;183:293–305.
4. Alnaqi AA, Moayedi H, Shahsavar A, Nguyen TK. Prediction of energetic performance of a building integrated photovoltaic/

thermal system thorough artificial neural network and hybrid particle swarm optimization models. Energy Convers Manag 2019;183:137–48.
5. Vakiloroaya V, Samali B, Fakhar A, Pishghadam KJ. A review of different strategies for HVAC energy saving. Energy Convers Manag. 2014;77:738–54.
6. Jung W, Jazizadeh FJ. Human-in-the-loop HVAC operations: a quantitative review on occupancy, comfort, and energy-efficiency dimensions. Appl Energy. 2019;239:1471–508.
7. Liu Z, Li W, Chen Y, Luo Y, Zhang L. Review of energy conservation technologies for fresh air supply in zero energy buildings. Appl Therm Eng. 2018;148:544–56.
8. Mardiana A, Riffat S. Review on physical and performance parameters of heat recovery systems for building applications. Renew Sustain Energy Rev. 2013;28:174–90.
9. Zeng C, Liu S, Shukla A. A review on the air-to-air heat and mass exchanger technologies for building applications. Renew Sustain Energy Rev. 2017;75:753–74.
10. Ziębik A, Gładysz P. Systems approach to energy and exergy analyses. Energy. 2018;165:396–407.
11. Shanazari E, Kalbasi R. Improving performance of an inverted absorber multi-effect solar still by applying exergy analysis. Appl Therm Eng. 2018;143:1–10.
12. Yang L, Du K, Zhang Z. Heat transfer and flow optimization of a novel sinusoidal minitube filled with non-Newtonian SiC/EG–water nanofluids. Int J Mech Sci. 2019. https://doi.org/10.1016/j.ijmecsci.2019.105310.
13. Costa VAF. On the exergy balance equation and the exergy destruction. Energy. 2016;116:824–35.
14. Sangi R, Müller D. Implementation of a solution to the problem of reference environment in the exergy evaluation of building energy systems. Energy. 2018;149:830–6.
15. Sangi R, Müller D. Exergy-based approaches for performance evaluation of building energy systems. Sustain Cities Soc. 2016;25:25–32.
16. Zhou Y. Evaluation of renewable energy utilization efficiency in buildings with exergy analysis. Appl Therm Eng. 2018;137:430–9.
17. Yari M, Kalbasi R, Talebizadehsardari P. Energetic-exergetic analysis of an air handling unit to reduce energy consumption by a novel creative idea. Int J Numer Methods Heat Fluid Flow. 2019;29:3959–75.
18. Amiri HA, Shafaghat R, Alamian R, Taheri SM, Shadloo MS. Study of horizontal axis tidal turbine performance and investigation on the optimum fixed pitch angle using CFD. Int J Numer Methods Heat Fluid Flow. 2019. https://doi.org/10.1108/HFF-05-2019-0447.
19. Hopp-Hirschler M, Shadloo MS, Nieken U. Viscous fingering phenomena in the early stage of polymer membrane formation. J Fluid Mech. 2019;864:97–140.
20. Nadooshan AA, Kalbasi R, Afrand M. Perforated fins effect on the heat transfer rate from a circular tube by using wind tunnel: an experimental view. Heat Mass Transf. 2018;54(10):3047–57.
21. Nguyen MQ, Shadloo MS, Hadjadj A, Lebon B, Peixinho J. Perturbation threshold and hysteresis associated with the transition to turbulence in sudden expansion pipe flow. Int J Heat Fluid Flow. 2019;76:187–96.
22. Piquet A, Zebiri B, Hadjadj A, Safdari Shadloo M. A parallel high-order compressible flows solver with domain decomposition method in the generalized curvilinear coordinates system. Int J Numer Methods Heat Fluid Flow. 2019. https://doi.org/10.1108/HFF-01-2019-0048.
23. Safdari Shadloo M. Numerical simulation of compressible flows by lattice Boltzmann method. Numer Heat Transfer Part A Appl. 2019;75(3):167–82.
24. Shenoy DV, Shadloo MS, Peixinho J, Hadjadj A. Direct numerical simulations of laminar and transitional flows in diverging pipes. Int J Numer Methods Heat Fluid Flow. 2019. https://doi.org/10.1108/HFF-02-2019-0111.
25. Kalbasi R, Afrand M, Alsarraf J, Tran M-D. Studies on optimum fins number in PCM-based heat sinks. Energy. 2019;171:1088–99.
26. Yang L, Du K. A comprehensive review on the natural, forced, and mixed convection of non-Newtonian fluids (nanofluids) inside different cavities. J Therm Anal Calorim. 2019. https://doi.org/10.1007/s10973-019-08987-y.
27. Yang L, Huang J, Ji W, Mao M. Investigations of a new combined application of nanofluids in heat recovery and air purification. Powder Technol. 2019. https://doi.org/10.1016/j.powtec.2019.10.053.
28. Yang L, Huang J, Mao M, Ji W. Numerical assessment of Ag-water nano-fluid flow in two new microchannel heatsinks: thermal performance and thermodynamic considerations. Int Commun Heat Mass Transf. 2020;110:104415. https://doi.org/10.1016/j.icheatmasstransfer.2019.104415.
29. Yang L, Ji W, Huang J, Xu G. An updated review on the influential parameters on thermal conductivity of nano-fluids. J Mol Liq. 2019;296:111780.
30. Yang L, Ji W, Zhang Z, Jin X. Thermal conductivity enhancement of water by adding graphene nano-sheets: consideration of particle loading and temperature effects. Int Commun Heat Mass Transf. 2019;109:104353.
31. Yang L, Mao M, Huang J, Ji W. Enhancing the thermal conductivity of SAE 50 engine oil by adding zinc oxide nano-powder: an experimental study. Powder Technol. 2019;356:335–41.
32. Yang L, Xu J, Du K, Zhang X. Recent developments on viscosity and thermal conductivity of nanofluids. Powder Technol. 2017;317:348–69.
33. Abedini E, Zarei T, Rajabnia H, Kalbasi R, Afrand M. Numerical investigation of vapor volume fraction in subcooled flow boiling of a nanofluid. J Mol Liq. 2017;238:281–9. https://doi.org/10.1016/j.molliq.2017.04.120.
34. Kalbasi R, Alemrajabi AA, Afrand M. Thermal modeling and analysis of single and double effect solar stills: an experimental validation. Appl Therm Eng. 2018;129:1455–65. https://doi.org/10.1016/j.applthermaleng.2017.10.012.
35. Kalbasi R, Salimpour MR. Constructal design of horizontal fins to improve the performance of phase change material rectangular enclosures. Appl Therm Eng. 2015;91:234–44. https://doi.org/10.1016/j.applthermaleng.2015.08.024.
36. Kalbasi R, Salimpour MR. Constructal design of phase change material enclosures used for cooling electronic devices. Appl Therm Eng. 2015;84:339–49. https://doi.org/10.1016/j.applthermaleng.2015.03.031.
37. Salimpour MR, Kalbasi R, Lorenzini G. Constructal multi-scale structure of PCM-based heat sinks. Contin Mech Thermodyn. 2017;29(2):477–91.
38. Khanmohammadi S, Saadat-Targhi M, Al-Rashed AAAA, Afrand M. Thermodynamic and economic analyses and multi-objective optimization of harvesting waste heat from a biomass gasifier integrated system by thermoelectric generator. Energy Convers Manag. 2019;195:1022–34. https://doi.org/10.1016/j.enconman.2019.05.075.
39. He W, Toghraie D, Lotfipour A, Pourfattah F, Karimipour A, Afrand M. Effect of twisted-tape inserts and nanofluid on flow field and heat transfer characteristics in a tube. Int Commun Heat Mass Transf. 2020;110:104440. https://doi.org/10.1016/j.icheatmasstransfer.2019.104440.
40. Mansouri H, Eghbali B, Afrand M. Producing multi-layer composite of stainless steel/aluminum/copper by accumulative roll

bonding (ARB) process. J Manuf Process. 2019;46:298–303. https://doi.org/10.1016/j.jmapro.2019.08.025.
41. Nassaj OR, Toghraie D, Afrand M. Effects of multi inlet guide channels on the performance of a cyclone separator. Powder Technol. 2019;356:353–72. https://doi.org/10.1016/j.powtec.2019.08.038.
42. Purjam M, Goudarzi K. High efficiency sub-critical carbon dioxide supplementary heat pump for low temperature climates (energy and exergy analysis). Renew Energy. 2019;133:166–76.
43. Chen L, Ge Y, Qin X, Xie Z. Exergy-based ecological optimization for a four-temperature-level absorption heat pump with heat resistance, heat leakage and internal irreversibility. Int J Heat Mass Transf. 2019;129:855–61.
44. Hu P, Hu Q, Lin Y, Yang W, Xing L. Energy and exergy analysis of a ground source heat pump system for a public building in Wuhan, China under different control strategies. Energy Build. 2017;152:301–12.
45. Compton M, Rezaie B. Enviro-exergy sustainability analysis of boiler evolution in district energy system. Energy. 2017;119:257–65.
46. Mosaffa A, Farshi LG, Ferreira CI, Rosen M. Energy and exergy evaluation of a multiple-PCM thermal storage unit for free cooling applications. Renew Energy. 2014;68:452–8.
47. Tyagi V, Pandey A, Buddhi D, Tyagi S. Exergy and energy analyses of two different types of PCM based thermal management systems for space air conditioning applications. Energy Convers Manag. 2013;69:1–8.
48. Rezaei M, Anisur M, Mahfuz M, Kibria M, Saidur R, Metselaar I. Performance and cost analysis of phase change materials with different melting temperatures in heating systems. Energy. 2013;53:173–8.
49. Baranski M, Fütterer J, Müller D. Distributed exergy-based simulation-assisted control of HVAC supply chains. Energy Build. 2018;175:131–40.
50. Fan B, Jin X, Fang X, Du Z. The method of evaluating operation performance of HVAC system based on exergy analysis. Energy Build. 2014;77:332–42.
51. Li Z, Shahsavar A, Al-Rashed AAAA, Kalbasi R, Afrand M, Talebizadehsardari P. Multi-objective energy and exergy optimization of different configurations of hybrid earth-air heat exchanger and building integrated photovoltaic/thermal system. Energy Convers Manag. 2019;195:1098–110.
52. Zhang K, Zhu Y, Liu J, Niu X, Yuan X. Exergy and energy analysis of a double evaporating temperature chiller. Energy Build. 2018;165:464–71.
53. Afrand M. Using a magnetic field to reduce natural convection in a vertical cylindrical annulus. Int J Therm Sci. 2017;118:12–23. https://doi.org/10.1016/j.ijthermalsci.2017.04.012.
54. Alsarraf J, Moradikazerouni A, Shahsavar A, Afrand M, Salehipour H, Tran MD. Hydrothermal analysis of turbulent boehmite alumina nanofluid flow with different nanoparticle shapes in a minichannel heat exchanger using two-phase mixture model. Physica A: Stat Mech Appl 2019;520:275–88.
55. Liu WI, Alsarraf J, Shahsavar A, Rostamzadeh M, Afrand M, Nguyen TK. Impact of oscillating magnetic field on the thermal-conductivity of water-Fe_3O_4 and water-Fe_3O_4/CNT ferro-fluids: experimental study. J Magn Magn Mater 2019;484:258–65.
56. Karimi A, Al-Rashed AAAA, Afrand M, Mahian O, Wongwises S, Shahsavar, A. The effects of tape insert material on the flow and heat transfer in a nanofluid-based double tube heat exchanger: two-phase mixture model. Int J Mech Sci 2019;156:397–409.
57. Liu WI, Al-Rashed AAAA, Alsagri AS, Mahmoudi B, Shahsavar A, Afrand M. Laminar forced convection performance of non-Newtonian water-CNT/Fe_3O_4 nano-fluid inside a minichannel hairpin heat exchanger: effect of inlet temperature. Powder Technol 2019;354:247–58.
58. Alsarraf J, Rahmani R, Shahsavar A, Afrand M, Wongwises S, Tran MD. Effect of magnetic field on laminar forced convective heat transfer of MWCNT–Fe_3O_4/water hybrid nanofluid in a heated tube. J Therm Anal Calorim 2019;137(5):1809–25.
59. Shahsavar A, Baseri MM, Al-Rashed AAAA, Afrand M. Numerical investigation of forced convection heat transfer and flow irreversibility in a novel heatsink with helical microchannels working with biologically synthesized water-silver nano-fluid. Int Commun Heat Mass Transf 2019;108:104324.
60. Liu W, Shahsavar A, Barzinjy AA, Al-Rashed AAAA, Afrand M. Natural convection and entropy generation of a nanofluid in two connected inclined triangular enclosures under magnetic field effects. Int Commun Heat Mass Transf 2019;108:104309.
61. Chen Z, Shahsavar A, Alrashed AAAA, Afrand M. The impact of sonication and stirring durations on the thermal conductivity of alumina-liquid paraffin nanofluid: an experimental assessment. Powder Technol 2020;360:1134–42.
62. Al-Rashed AAAA, Shahsavar A, Akbari M, Toghraie D, Akbari M, Afrand M. Finite volume simulation of mixed convection in an inclined lid-driven cavity filled with nanofluids: effects of a hot elliptical centric cylinder, cavity angle and volume fraction of nanoparticles. Physica A: Stat Mech Appl 2019;527:121122.
63. Shahsavar A, Bagherzadeh SA, Mahmoudi B, Hajizadeh A, Afrand M, Nguyen TK. Robust weighted least squares support vector regression algorithm to estimate the nanofluid thermal properties of water/graphene oxide-silicon carbide mixture. Physica A: Stat Mech Appl 2019;525:1418–28.
64. Alsarraf J, Shahsavar A, Khaki M, Ranjbarzadeh R, Karimipour A, Afrand M. Numerical investigation on the effect of four constant temperature pipes on natural cooling of electronic heat sink by nanofluids: a multifunctional optimization. Adv Powder Technol 2019;5:5–9.
65. Monfared M, Shahsavar A, Bahrebar MR. Second law analysis of turbulent convection flow of boehmite alumina nanofluid inside a double-pipe heat exchanger considering various shapes for nanoparticle. J Therm Anal Calorim 2019;135(2):1521–32.
66. Al-Rashed AAAA, Shahsavar A, Entezari S, Moghimi MA, Adio SA, Nguyen TK. Numerical investigation of non-Newtonian water-CMC/CuO nanofluid flow in an offset strip-fin microchannel heat sink: thermal performance and thermodynamic considerations. Appl Therm Eng 2019;155:247–58.
67. Shahsavar A, Rahimi Z, Salehipour H. Nanoparticle shape effects on thermal-hydraulic performance of boehmite alumina nanofluid in a horizontal double-pipe minichannel heat exchanger. Heat Mass Transf 2019;55(6):1741–51.
68. Liu X, Mohammed HI, Ashkezari AZ, Shahsavar A, Hussein AK, Rostami S. An experimental investigation on the rheological behavior of nanofluids made by suspending multi-walled carbon nanotubes in liquid paraffin. J Mol Liq 2020;300:112269.
69. Dovjak M, Shukuya M, Krainer A. Connective thinking on building envelope–Human body exergy analysis. Int J Heat Mass Transf. 2015;90:1015–25.
70. Buyak N, Deshko V, Sukhodub I. Buildings energy use and human thermal comfort according to energy and exergy approach. Energy Build. 2017;146:172–81.
71. Li Z, Al-Rashed AA, Rostamzadeh M, Kalbasi R, Shahsavar A, Afrand M. Heat transfer reduction in buildings by embedding phase change material in multi-layer walls: effects of repositioning, thermophysical properties and thickness of PCM. Energy Convers Manag. 2019;195:43–56.
72. Razmara M, Maasoumy M, Shahbakhti M, Robinett R III. Optimal exergy control of building HVAC system. Appl Energy. 2015;156:555–65.
73. Khalid F, Dincer I, Rosen M. Development and analysis of sustainable energy systems for building HVAC applications. Appl Therm Eng. 2015;87:389–401.

74. Sayadi S, Tsatsaronis G, Morosuk T. Dynamic exergetic assessment of heating and cooling systems in a complex building. Energy Convers Manag. 2019;183:561–76.
75. Caliskan H, Lee D-Y, Hong H. Enhanced thermodynamic assessments of the novel desiccant air cooling system for sustainable energy future. J Clean Prod. 2019;211:213–21.
76. Bejan A. Advanced engineering thermodynamics. Hoboken: Wiley; 2016.
77. ASHRAE Handbook. HVAC systems and equipment. American Society of Heating, Refrigerating, and Air Conditioning Engineers, Atlanta, GA. 1996; 1–10.
78. Besant RW, Simonson CJ. Chapter 44: Air-to-air energy recovery. ASHRAE handbook: HVAC systems and equipment. 2000